Modeling of Mechanical Response and Progressive Failure of Tri-axially Woven SiC$_f$-SiC Composites

S. G. Kulkarni[1], <u>X.-L. Gao</u>[2],*

[1] Department of Mechanical Engineering, Texas A&M University, College Station, TX 77843

[2] Department of Mechanical Engineering, University of Texas at Dallas, Richardson, TX 75080-3021

* Corresponding author: Xin-Lin.Gao@utdallas.edu

Abstract   Effective properties and progressive failure of SiC matrix composites reinforced by tri-axially woven SiC fibers (SiC$_f$) (as a fabric) are predicted. Three different orientations of the woven fabric are considered in geometrical modeling, including −60°-0°-60°, −55°-0°-55° and −45°-0°-45°. Three-dimensional unit cells with the matrix reinforced by the fabrics in such orientations are constructed and used. Homogenization analyses are carried out using the finite element method (FEM). It is found that the −60°-0°-60° fabric orientation provides the highest values for the effective elastic moduli, while the −45°-0°-45° orientation gives the lowest values. The effective properties obtained are then used to conduct a progressive failure analysis of the SiC$_f$-SiC composite subjected to uni-axial tensile loading. The progressive failure analysis incorporates both geometrical and material non-linearities, and describes the progressive damage induced by crack initiation and propagation through a material degradation model. The Tsai-Wu failure criterion is used, and a two-parameter Weibull distribution is employed to account for the changes in strength with increasing specimen volume. Based on this progressive failure analysis, stress-strain curves for the SiC$_f$-SiC composites are plotted, and the −60°-0°-60° orientation is found to have the smallest deformations at given loads.

Key words   Woven composite, Effective property, Homogenization, Progressive failure analysis, SiC$_f$-SiC

1. Introduction

SiC fabric reinforced SiC matrix composites have emerged as a class of strong, radiation-resistant, high-temperature structural materials that are suitable and ready for nuclear fusion applications [1]. SiC has been used as a nuclear fuel cladding material since it offers greater strength at high temperatures than conventional zirconium alloys. SiC has excellent irradiation tolerance, low chemical reactivity, and low tritium permeability [2].

Textile composites represent a class of advanced materials that are reinforced by fabric preforms. The smallest constituent of a textile composite is a fiber. A yarn is an assembly of fibers. Yarns are generally used as unit elements to form fabrics. A tri-axially woven fabric has three sets of yarns forming equilateral triangles at the intersections. Tri-axially woven fabrics have no weak dimension or bias and offer high resistance to shear or tear. They also have the ability to accommodate compound curvatures and are therefore suitable for molded manufacturing. These features make tri-axially woven fabric composites ideal for cladding tube applications, where high temperatures can cause considerable normal and shear stresses in cladding tubes.

Effective properties and progressive failure of tri-axially woven SiC_f-SiC ceramic matrix composites are studied in the current paper using micromechanics and the finite element method. Representative volume elements are identified for three different fabric configurations. The matrix material is regarded as isotropic, while the fabric yarns are treated as transversely orthotropic. Homogenization analyses are performed to determine effective properties, and progressive failure studies are then conducted to obtain stress-strain curves for the SiC_f-SiC composites.

2. Unit Cells

Most fabrics are woven with two sets of orthogonal yarns called the warp and weft yarns [3]. This is known as bi-axial weaving. The most common tri-axially woven fabrics are the ones where the fiber yarns are arranged in the +45°, 0°, and −45° orientation. However, tri-axially woven fabrics can be made with any orientation ranging from ±20° and ±70°. In the current study, three different orientations are considered to evaluate effective properties of tri-axially woven SiC_f-SiC ceramic matrix composites. The three orientations considered are −60°, 0°, +60°; −55°, 0°, +55°; and −45°, 0°, +45°. For each of these three configurations, a repetitive structure can be taken as a unit cell. The cross section of each yarn is assumed to be lenticular, as was done by others. Figure 1 shows a unit cell of the composite reinforced by the −60°- 0°-60° fabric.
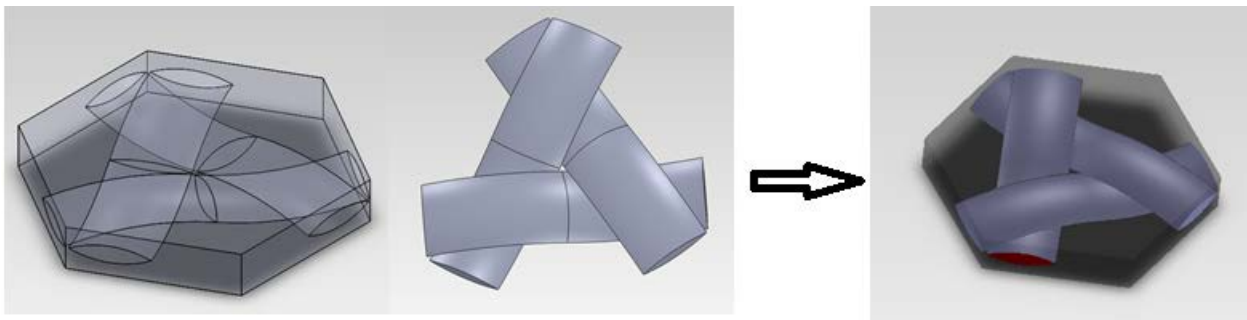
Figure 1. Unit cell of a tri-axially woven fabric reinforced composite

The tri-axially woven fabric of SiC fibers will serve as the reinforcement of the ceramic matrix composite. It can be seen from Figs. 1 and 2 that the tri-axially woven yarns form equilateral triangles and hexagonal holes, which change in size with the yarn orientation, as shown in Fig. 3. For SiC_f-SiC composites, the matrix and fibers are made from the same material. Therefore, the matrix adds considerable stiffness to the composite and the matrix material in the holes and triangles may not be neglected in a homogenization analysis. In constructing the models, the matrix pocket and woven fabric are first generated separately. The fabric and matrix pocket are then assembled to yield the composite unit cell, as shown in Fig. 1. Bonded contact between the matrix and the fabric is assumed to represent perfect bonding.
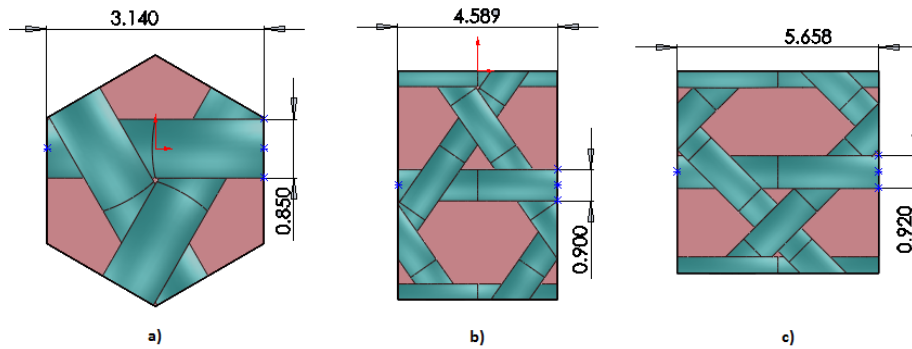
Figure 2. a) Hexagonal unit cell for the −60°-0°-60° fabric configuration; b) rectangular unit cell for the −55°-0°-55° configuration; and c) rectangular unit cell for the −45°-0°-45° configuration

In the homogenization analysis, the matrix material is considered as isotropic, and the fiber yarn is regarded as a transversely isotropic material that has five independent elastic constants.
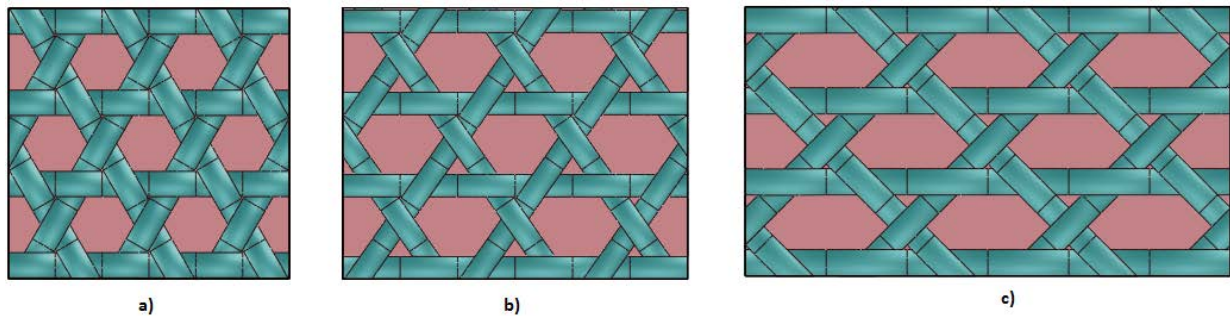
Figure 3. Composite specimens: a) −60°-0°-60°, b) −55°-0°-55°, and c) −45°-45°-45°

3. Finite Element Analysis

A finite element analysis is performed on each of the three unit cells identified in Fig. 2 to obtain effective properties of the SiC$_f$-SiC ceramic matrix composites using the commercial software package ANSYS. The material properties used are listed in Table 1, which are taken from [4]. The unit cell is meshed using three-dimensional, 10-node solid elements, as shown in Fig. 4. These elements are well suited to model irregular geometries. Each of these solid elements has three degrees of freedom at every node: translations in the X, Y and Z nodal directions.
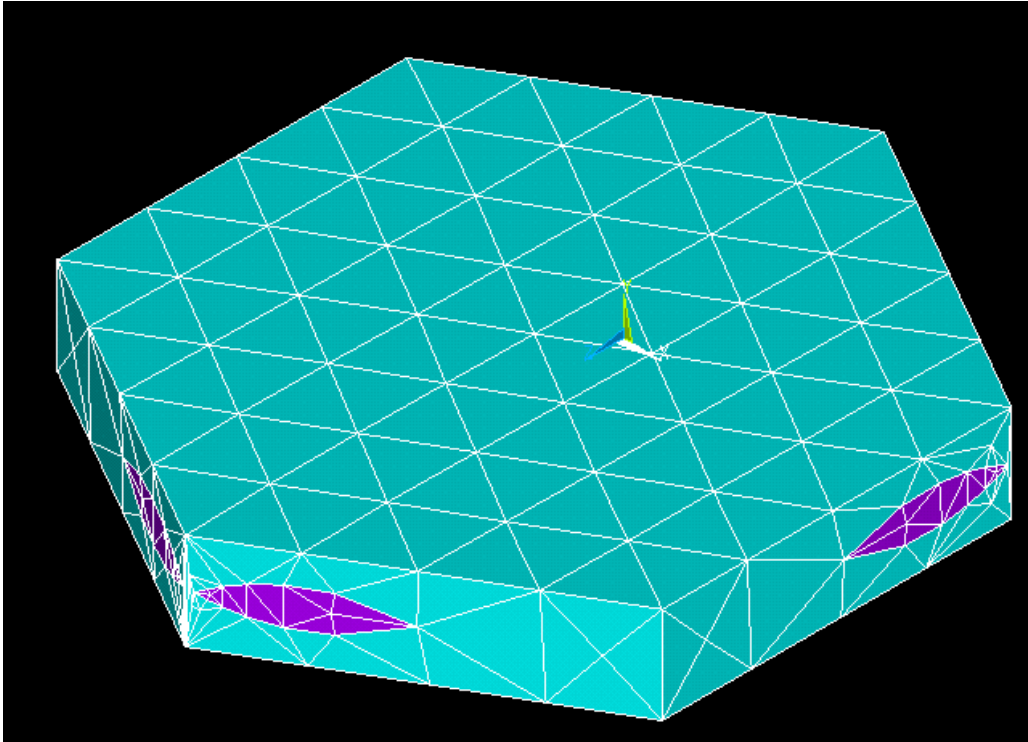
Figure 4. Finite element mesh for the unit cell shown in Fig. 2a)

Table 1. Properties of the matrix and yarn [4]

Material Properties	Matrix	Yarn
E_{11}	251 GPa	221 GPa
E_{22}	251 GPa	219.8 GPa
E_{33}	251 GPa	219.8 GPa
v_{12}	0.16	0.214
v_{23}	0.16	0.193
v_{13}	0.16	0.193
G_{12}	108 GPa	108 GPa
G_{23}	108 GPa	90.4 GPa
G_{31}	108 GPa	90.4 GPa
α_1	$4\times10^{-6}\,\mathrm{K}^{-1}$	$3.43\times10^{-6}\,\mathrm{K}^{-1}$
α_2	$4\times10^{-6}\,\mathrm{K}^{-1}$	$3.38\times10^{-6}\,\mathrm{K}^{-1}$
α_3	$4\times10^{-6}\,\mathrm{K}^{-1}$	$3.38\times10^{-6}\,\mathrm{K}^{-1}$

3.1 Periodic Boundary Conditions

In modeling uniaxial and biaxial tensile tests, displacement boundary conditions are frequently used. Since a representative volume element (RVE) is cut out of an infinite composite, spatially periodic

boundary conditions should be applied to ensure that the predicted properties of the RVE represent those of the composite [5-7].

The periodic boundary conditions are implemented using the CE option available in ANSYS. Deformations of two unit cells subject to periodic boundary conditions are shown in Fig. 5.
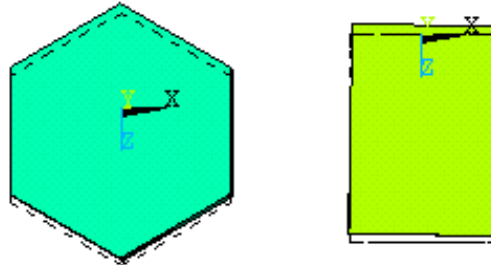
Figure 5. Deformations of hexagonal and rectangular unit cells under periodic boundary conditions

3.2 Model Validation

The model validation is carried out by comparing the simulation results with the experimental data obtained in Fujita et al. [8] for a tri-axially woven carbon fiber reinforced epoxy matrix composite. As shown in Fig. 6, the effective tensile modulus predicted by the current unit-cell based model using periodic boundary conditions agrees well with the experimental value of Fujita et al. [8], thereby supporting the model.
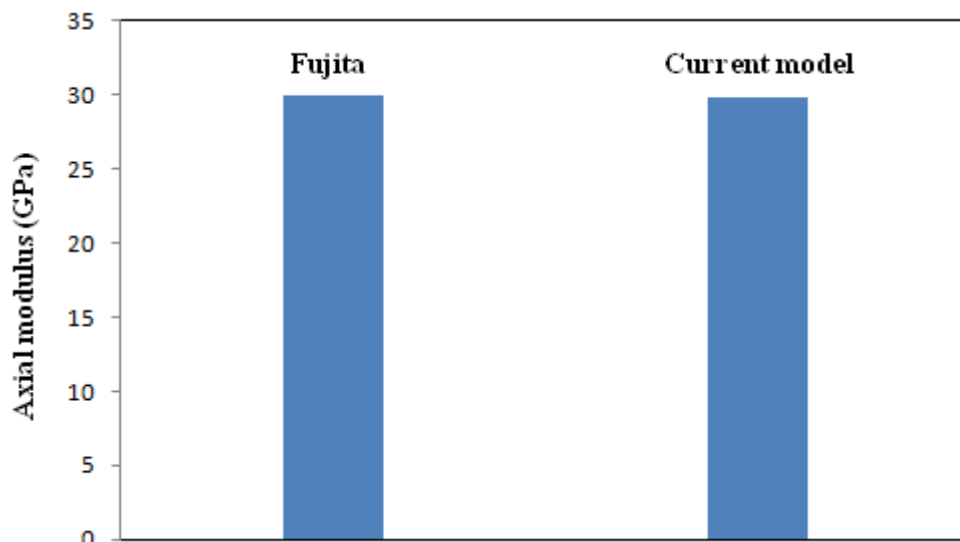
Figure 6. Comparison with the experimental result of Fujita et al. [8]

3.3 Effective Properties

With the unit-cell based FE model validated, simulations are performed using the three unit cell configurations shown in Fig. 2 and the constituent properties listed in Table 1. The in-plane effective properties obtained in the simulations are given in Table 2.

Table 2**.** Effective properties for different fabric orientations

Boundary Conditions	Effective Properties	60° Orientation	55° Orientation	45° Orientation
	E_{11} (GPa)	285.857	244.333	239.8992
Periodic Boundary Conditions	E_{22} (GPa)	252.587	242.992	226.224
	E_{33} (GPa)	252.587	242.992	226.224
	v_{12}	0.1713	0.15266	0.15814
	G_{12} (GPa)	105.26	98.644	98.111

The fiber volume fraction for all the three unit cells is kept equal (within ±2%). It can be seen from Table 2 that the −60°-0°-60° orientation has the highest values of the elastic moduli, while the −45°-0°-45° orientation has the lowest values.

4. Progressive Failure Analysis

Catastrophic failure of a composite structure does not occur at the material failure strength. Composite structures typically fail after propagation or accumulation of localized damages such as matrix cracking, fiber breakage, and fiber-matrix debonding. These mechanisms ultimately lead to the loss of load-carrying ability of the composite structure. Hence, progressive failure analysis is needed to simulate damage propagation and ultimately failure of a composite structure. In the current work, a progressive failure analysis is carried out for uniaxial tension tests. Stress-strain curves are determined for all three fabric reinforcement configurations.

The procedure for the progressive failure analysis is as follows:
a. Each composite specimen (see Fig. 3) is subjected to uniaxial tension. Before the initiation of the first failure, only geometrical nonlinearities (large deformations) are accounted for.
b. After each load increment, stresses at each node are evaluated against a failure criterion.
c. If there is no failure initiation, load is further increased.
d. Upon failure initiation at a node, the elastic modulus in the loading direction is degraded for all elements connected to that node using a material degradation model.
e. The load is then increased.

This procedure is repeated until the specimen loses its load-carrying capability or up to a certain strain level.

5. Failure Criterion and Material Degradation Model

The Tsai-Wu failure model [9,10] is used as the failure criterion. Failure analysis by comparing with a failure criterion is deterministic in nature [11]. In such an analysis, the risk of fracture remains unknown. Therefore, probabilistic fracture analysis is required for better predictions. For a brittle material like SiC, its properties display strong scattering. Brittle materials also show a pronounced

decrease in strength with increasing specimen volume owing to defect distributions. As the material volume increases, the occurrence probability of critical defects increases. Probabilistic analysis takes into account uncertainties in material properties, loading conditions, and defect distributions. In the current work, these uncertainties are accounted for by using the following two-parameter Weibull distribution [4,11]:

$$P_f = 1 - \exp\left[-\frac{V}{V_0}\left(\frac{\sigma - \sigma_u}{\sigma_0} \right)^m \right],$$ (1)

where P_f is the fracture probability, V is the specimen volume under consideration, σ is the stress induced in the specimen, V_0 and σ_0 are normalization parameters, m is the Weibull shape parameter, and σ_u is the threshold stress below which the fracture probability is zero. For SiC, m can be taken as 7.6, σ_0 as 270 MPa, V_0 as 65.49 mm^3, and σ_u as zero [1]. P_f gives the failure probability for the specimen volume V under stress σ. For every load increment, P_f is evaluated for each individual element. Failure occurs if $P_f = 0.99$.

When failure is detected at any node in the composite, the elastic properties are reduced for all the surrounding elements containing that node using a material degradation model. The crack band theory developed for concrete [12] is adopted as the material degradation model. According to the crack band theory, the post failure relation between the normal stresses σ_x, σ_y, σ_z and the normal strains ε_x, ε_y, ε_z can be written as

$$\begin{Bmatrix} \varepsilon_x \\ \varepsilon_y \\ \varepsilon_z \end{Bmatrix} = \begin{bmatrix} C_{11}\mu^{-1} & C_{12} & C_{13} \\ & C_{22} & C_{23} \\ symmetric & & C_{33} \end{bmatrix} \begin{Bmatrix} \sigma_x \\ \sigma_y \\ \sigma_z \end{Bmatrix},$$ (2)

where μ is a cracking parameter, and C_{ij} are compliance constants. The cracking parameter μ depends on the material properties and strain level and is given by

$$\frac{1}{\mu} = \frac{E}{-E_t} \frac{\varepsilon_x}{\varepsilon_0 - \varepsilon_x},$$ (3)

where ε_x is the strain in the loading direction, E is Young's modulus, E_t is the tangent (softening) modulus, and ε_0 is a constant. Note that $\mu = 1$ in an un-cracked material and $\mu = 0$ is a continuously cracked material. After failure is detected, Young's modulus in the loading direction is degraded by a factor μ, while the other properties remain the same. When a crack is introduced in the composite, no normal stress can be transferred across the crack surfaces. However, after the load is increased, the stresses in the surrounding region still increase because of the load transfer from undamaged parts of the composite. Therefore, multiple cracks can occur in one element. This simulation is continued until the composite loses its ability to carry any more load.

6. Stress-Strain Curves

The properties obtained in the progressive failure analysis are used to plot stress-strain curves for all

three configurations, as shown in Figs. 7 and 8. These are based on the uniaxial tension tests of the composite specimens displayed in Fig. 3.
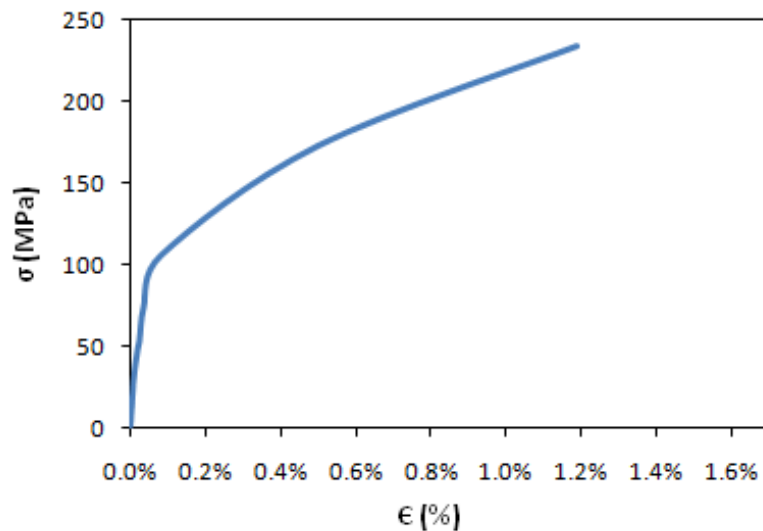
Figure 7. Stress-strain curve from the −60°-0°-60° specimen
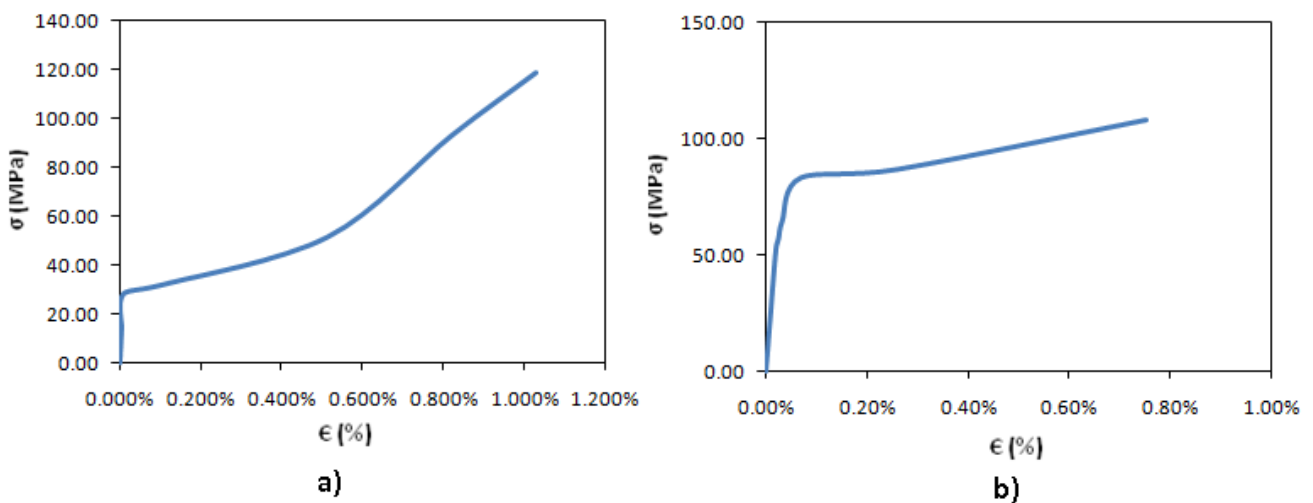
Figure 8. a) Stress-strain curves from a) the −55°-0°-55° specimen and b) the −45°-0°-45° specimen

The progressive failure analysis has revealed that crack initiation occurs first in the transverse direction and at the fabric-matrix interfaces. The linear material behavior ends with the initiation of cracks. The material degradation model discussed in Section 5 is then applied to introduce Mode I cracks in the mesh. After the cracks have been introduced, stresses in the composite specimen may increase or decrease in the next immediate load increment, since no normal stress can be transferred across the crack surfaces. However, as the load is further increased, the stresses begin to increase because of the stress transfer from the surrounding undamaged parts of the composite.

It can be seen from Figs. 7 and 8 that the −60°-0°-60° configuration has the smallest deformations at given loads.

Acknowledgements

References

[1] L.L. Snead, T. Nozawa, Y. Katoh, T.S. Byun, S. Kondo, D.A. Petti, Handbook of SiC properties for fuel performance modelling. J. Nuclear Mater., 371(2007) 329–377.

[2] Y. Katoh, L.L. Snead, C.H. Henager Jr., A. Hasegawa, A. Kohyama, B. Riccardi, H. Hegeman, Current status and critical issues for development of SiC composites for fusion applications. J. Nuclear Mater., 367-370 (2007) 659–671.

[3] X.-L. Gao, S. Mall, A two-dimensional rule-of-mixtures micromechanics model for woven fabric composites. ASTM J. Compos. Tech. Res., 22 (2000), 60–70.

[4] H. Ismar, F. Schroter, F. Streicher, Modeling and numerical simulation of the mechanical behavior of woven SiC/SiC regarding a three dimensional unit cell. Comput. Mater. Sci., 19 (2000) 320–328.

[5] K. Li, X.-L. Gao, G. Subhash, Effects of cell shape and cell wall thickness variations on the elastic properties of two-dimensional cellular solids. Int. J. Solids Struct., 42 (2005) 1777–1795.

[6] K. Li, X.-L. Gao, G. Subhash, Effects of cell shape and strut cross-sectional area variations on the elastic properties of three-dimensional open-cell foams. J. Mech. Phys. Solids, 54 (2006) 783–806.

[7] Z. Xia, Y. Zhang, F. Ellyin, A unified periodical boundary conditions for representative volume elements of composites and applications. Int. J. Solids Struct., 40 (2003) 1907–1921.

[8] A. Fujita, H. Hamada, Z. Maekawa, Tensile properties of carbon fiber triaxial woven fabric composites. J. Compos. Mater., 27 (1993) 1428–1441.

[9] S.W. Tsai, E.M. Wu, A general theory of strength for anisotropic materials. J. Compos. Mater., 5(1971) 58–80.

[10] S.S. Zhou, X.-L. Gao, G.W. Griffith, Analysis and structural optimization of a three-layer composite cladding tube under thermo-mechanical loads. ASME J. Eng. Mater. Tech., 134 (2012) 031001-1–12.

[11] D. Gross, T. Seelig, Fracture Mechanics: with an Introduction to Micromechanics, Springer-Verlag, Berlin, Germany, 2006.

[12] Z.P. Bazant, B.H. Oh, Crack band theory for fracture of concrete. Mater. Struct., 16 (1983) 155–177.